ProNGF increases breast tumor aggressiveness through functional association of TrkA with EphA2

Romain Lévêque, Cyril Corbet, Léo Aubert, Matthieu Guilbert, Chann Lagadec, Eric Adriaenssens, Jérémy Duval, Pascal Finetti, Daniel Birnbaum, Nicolas Magné, et al.

ProNGF increases breast tumor aggressiveness through functional association of TrkA with EphA2

Lévêque Romain[1,2,¥], Corbet Cyril[1,2,¥,§], Aubert Léo[1,2,¥], Guilbert Matthieu[1,2], Lagadec Chann[1], Adriaenssens Eric[1,2], Duval Jérémy[1,2], Finetti Pascal[3], Birnbaum Daniel[3], Magné Nicolas[4,5], Chopin Valérie[2,6], Bertucci François[3], Le Bourhis Xuefen[1,2,#] & Toillon Robert-Alain[1,2,#,*]

[1] Inserm, U908, F-59000 Lille, France,
[2] Univ. Lille, U908 - CPAC - Cell plasticity and Cancer, F-59000 Lille, France,
[3] Département d'Oncologie Moléculaire, Institut Paoli-Calmette, CRCM, UMR1068 Inserm, UMR7258 CNRS, Aix-Marseille Université, 13273 Marseille, France,
[4] Département de Radiothérapie, Institut de Cancérologie Lucien Neuwirth, 42270 Saint Priest en Jarez, France,
[5] Radiobiologie Cellulaire et Moléculaire, EMR3738 - Equipe 4, Faculté de Médecine Lyon-Sud, 69000 Lyon, France,
[6] Université de Picardie, 80000 Amiens, France.

[¥] The authors have equally contributed to this work.
Co-senior authors.
[§] Current address: Pole of Pharmacology and Therapeutics (FATH), Institut de Recherche Expérimentale et Clinique (IREC), UCLouvain, 53 Avenue Mounier B1.53.09, B-1200 Brussels, Belgium.
***** Corresponding author: Prof. Robert-Alain Toillon, INSERM U908 "Cell Plasticity & Cancer", Bâtiment SN3, 3ème étage, Cité scientifique, Université Lille 1, 59655 Villeneuve d'Ascq, France. Phone: +33 (0)3 20 43 65 59;
E-mail: robert-alain.toillon@univ-lille.fr

Running title: TrkA/EphA2 functional association in breast cancer cells

Keywords: EphA2, TrkA, proNGF, breast cancer

Financial support

This work was supported by grants from the “Ligue Nationale Contre le Cancer”, “Fondation ARC pour la recherche sur le cancer”, “Groupement des Entreprises Françaises dans la Lutte contre le Cancer (GEFLUC)” and the SIRIC Oncolille.

Abstract: 180 words

Word count: 3775 words (+ 41 references)

Number of figures/tables: 6 figures + 1 table

Highlights

- EphA2 is a key element of proNGF signaling in breast cancer cells
- ProNGF-induced Src activation through EphA2 is independent of TrkA phosphorylation
- TrkA/EphA2 PLA signal is associated with decrease of overall survival in breast cancer

Abstract

ProNGF expression has been linked to several types of cancers including breast cancer, and we have previously shown that proNGF stimulates breast cancer invasion in an autocrine manner through membrane receptors sortilin and TrkA. However, little is known regarding TrkA-associated protein partners upon proNGF stimulation. By proteomic analysis and proximity ligation assays, we found that proNGF binding to sortilin induced sequential formation of the functional sortilin/TrkA/EphA2 complex, leading to TrkA-phosphorylation dependent Akt activation and EphA2-dependent Src activation. EphA2 inhibition using siRNA approach abolished proNGF-stimulated clonogenic growth of breast cancer cell lines. Combinatorial targeting of TrkA and EphA2 dramatically reduced colony formation *in vitro*, primary tumor growth and metastatic dissemination towards the brain *in vivo*. Finally, proximity ligation assay in breast tumor samples revealed that increased TrkA/EphA2 proximity ligation assay signals were correlated with a decrease of overall survival in patients.

All together, these data point out the importance of TrkA/EphA2 functional association in proNGF-induced tumor promoting effects, and provide a rationale to target proNGF/TrkA/EphA2 axis by alternative methods other than the simple use of tyrosine kinase inhibitors in breast cancer.

1. Introduction

Elevated levels of pleiotropic growth factors and their cognate receptor tyrosine kinases (RTK) as well as mutated receptors actively participates to cancer progression and resistance to targeted therapies using tyrosine kinase inhibitors [1,2]. Tumor resistance to specific tyrosine kinase inhibitors may be due to complex cross-talk in terms of receptor interactions and their redundant or diversified downstream signaling partners [1,2]. This underlies the need to better characterize growth factor signaling and RTK cooperation in order to optimize such therapies.

In the case of TrkA signaling networks, elicited by nerve growth factor (NGF), several co-receptors such as $p75^{NTR}$, ErbB2, and Ret-5 [3–5] have been reported to modulate TrkA-induced biological effects. Moreover, sortilin is known to be involved in TrkA signaling networks under proNGF (precursor of NGF) stimulation. Sortilin, a member of the Vps10p-domain proteins, is mainly known to be involved in vesicular trafficking but it also acts as a membrane receptor for neurotensin and proneurotrophins [6,7]. Although recombinant proNGF has been described to directly bind to sortilin, $p75^{NTR}$ and TrkA, it has been found that, in neuron cells, proNGF induces sortilin/$p75^{NTR}$ complex formation, leading to apoptotic cell death [8]. Further study showed that high ratio between $p75^{NTR}$ and TrkA stimulates proNGF-induced neuron apoptosis, while low ratio between $p75^{NTR}$ and TrkA stimulates proNGF-induced survival [9]. ProNGF is also associated with non-neuronal malignancies and its expression has been reported in melanoma, prostate, breast and thyroid cancers [10–13]. In melanoma, proNGF can stimulate cancer cell invasion through $p75^{NTR}$ [12] while in prostate cancer, its expression correlates with aggressiveness and nerve infiltration into the tumor site [11]. In breast cancer, we previously reported high levels of proNGF are correlated with lymph node invasion

[10]. In addition, proNGF stimulates breast cancer cell invasion through sortilin and TrkA receptors, independently of $p75^{NTR}$, leading to the subsequent activation of Src and Akt signaling pathways [10].

Despite the tumor-promoting effects of proNGF, associated signaling pathways still remain fragmentary. Here, we identified EphA2, a membrane receptor tyrosine kinase, as a key element of the proNGF signaling in breast cancer cells. Moreover, increased TrkA/EphA2 proximity ligation assay signals were correlated with a decrease of overall survival in breast cancer patients, further pointing out the importance of TrkA/EphA2 functional association in proNGF-mediated tumor progression. Thus, our results provide a rationale to target proNGF/TrkA/EphA2 axis as a promising therapeutic strategy in breast cancer.

2. Materials and Methods

2.1. Cell culture

All breast cancer cell lines were acquired from the American Type Culture Collection (ATCC) except for SUM159-PT, which is from Asterand Bioscience. MDA-MB-231 breast cancer cells stably overexpressing HA-tagged native TrkA (MDA-MB-231 HA-TrkA) or a kinase-dead TrkA were established as previously described [10]. Cells were maintained in Eagle's Minimal Essential Medium (Life Technologies) (MDA-MB-231 and MCF-7 cells), or RPMI 1640 medium (Life Technologies) (HCC-1954, T-47D) supplemented with 10 % inactivated FBS (Fetal Bovine Serum) (Hyclone), 2 mM L-glutamine, 1 % non-essential amino acids, 40 UI/ml penicillin, 40 µg/ml streptomycin, 50 µg/ml gentamycin and ZellShield™ (Biovalley) at 37°C in 5 % CO_2-humidified atmosphere. SUM159-PT were grown in Ham's F12 nutrient mix supplemented with 5 % FBS, 10 mM HEPES, 0.1 % insulin, 1 mg/ml hydrocortisone, 40 UI/ml penicillin, 40 µg/ml streptomycin, 50 µg/ml gentamycin and ZellShield™ (Biovalley) at 37°C in 5 % CO_2-humidified atmosphere. Before treatment, cells were rinsed twice with PBS, left for 24h in culture medium supplemented with 0.1 % FBS, and then treated with recombinant human non-cleavable proNGF (denoted as proNGF and used at 0.5 nM in all the experiments) (Alomone Labs) or recombinant human mature NGF at 16 nM (Alomone labs). For some experiments, cells were pre-incubated for 1h with the TrkA pharmacological inhibitor K252a (10 nM, Calbiochem) or neurotensin (1 µM, R&D systems).

2.2. Transfection

Tumor cells were transfected with 2 nM siRNA using INTERFERin™ transfection reagent (Polyplus transfection) following the manufacturer's instructions. The siRNA sequences used against EphA2 were: GCAAGGAAGUGGUACUGCUGGACUU

(from Eurogentec) or GCGUAUCUUCAUUGAGCUCAA [14] compared to a control siRNA sequence (siGFP) GAUGAACUUCAGGGUCAGCTT. For TrkA, a pool of three siRNA sequences (Eurogentec) was used: GAACCUGACUGAGCUCUAC, UGGAGUCUCUCUCCUGGAA and GCUGCAGUGUCAUGGGCAA.

2.3. Immunoprecipitation and Western blot analysis

Immunoprecipitation and Western blotting experiments were carried out as previously reported [15]. The primary antibodies used for Western blotting were: anti-sortilin (#612101, BD Biosciences), anti-TrkA (ANT-018, Alomone Labs), anti-EphA2 (clone 1E3, Abnova), anti-HA (Covance), anti-phospho-Akt (Ser-473) (#9271), anti-pan-Akt (#4691), anti-phospho-Src (Tyr-416) (#2105), anti-Src (#2109) and anti-phospho-TrkA (Tyr-674/675) (#4621) (Cell Signaling Technology). For immunoprecipitation studies, anti-HA (12CA5, Roche), anti-sortilin (BAF2934, R&D Systems) and anti-EphA2 (clone C-20, Santa Cruz Biotechnologies) were used.

2.4. Nano-LC-MS/MS Q-Star analysis

MDA-MB-231 HA-TrkA cells were treated with proNGF for 5 or 30 min. Total cell lysates were subjected to immunoprecipitation using anti-HA (Covance). Immunoprecipitated proteins were then separated by 10 % SDS-PAGE. After colloidal Coomassie blue staining, bands, which intensities were increased under proNGF stimulation, were cut and peptide digests were extracted from the 1-D gel band and nanoLC-nanoESI-MS/MS analyses were performed on a hybrid quadrupole time-of-flight mass spectrometer (Q-Star, Applied Biosystems) equipped with a nano-electrospray ion source coupled with a nano high pressure

liquid chromatography system (LC Packings Dionex) as previously described [16]. Identified proteins were classified by Panther software (http://www.pantherdb.org).

2.5. *In situ* proximity ligation assay (PLA)

Cells grown on acid-washed eight-well glass slides (10^4 cells per well) (Thermo Scientific) in appropriate medium with 5 or 10 % FBS for 24h. After treatment, paraformaldehyde-fixed cells were incubated with 4 % BSA (1h, 20°C) followed by overnight incubation with primary antibodies [mouse anti-HA, 1:50 (Covance); goat anti-sortilin, 1:50 (R&D systems); rabbit anti-EphA2, 1:100 (Cell Signaling Technology), mouse anti-TrkA, 1:50 (Alomone Labs)]. PLA was performed as recommended by manufacturer's instructions. Briefly, slides were incubated with secondary antibodies complexed with complementary nucleotide sequences for 2h. The formed DNA circle, resulting from complementary nucleotides was then amplified using fluorescent oligonucleotides. Nuclei were counterstained with Hoechst 33258 (Sigma-Aldrich) and samples were mounted with fluorescence mounting medium (Dako). PLA images (fluorescent red dots) were acquired using a fluorescence microscope (100X oil immersion objective, $\lambda_{excitation}$: 562 nm, $\lambda_{emission}$: 624 nm, microscope Eclipse Ti; Nikon) and analyzed with NIS-Elements BR software (Nikon) and Image J.

Tissue microarrays were from SuperBioChips (CBA4) and US BioMax (HBre-Duc150Sur01) allowing analysis in 189 individual tumor samples. For PLA in paraffin-embedded patient tumor samples, primary antibodies anti-TrkA (ANT-018, Alomone Labs) and anti-EphA2 (AF3035, R&D systems) were incubated overnight at 4°C. Subsequent steps were done according to the manufacturer's instructions. Briefly, slides were incubated with secondary antibodies complexed with complementary nucleotide sequences for 2h. The formed DNA circle, resulting from

complementary nucleotides was then amplified using oligonucleotides labeled with horseradish peroxidase. PLA signal was evaluated according to the number of dots per cell and the number of stained cells in a double-blind analysis (by TRA and DJ). PLA signal <2 dots/cell was considered as low, PLA signal between 2-10 dots/cell was considered as medium, PLA signal >10 dots/cell was considered as high. Kaplan-Meier curves were obtained by using GraphPad Prism software.

2.6. Clonogenic cell growth

Clonogenic assays were performed as previously described [15]. After siRNA transfection, 2000 cells were seeded in 35 mm Petri dishes and treated with proNGF for 10 days. Colonies were then stained with crystal violet before counting.

2.7. *In vivo* experiments

All the experiments involving mice received the approval of the local ethic committee and were carried out according to French national animal care regulations. MDA-MB-231 HA-TrkA cells ($3x10^6$) were subcutaneously injected into six-week old female SCID mice. Two weeks after cell injection, mice were randomized into four groups (n=7), and were treated a total of three times at 3-day intervals. Lestaurtinib (CEP-701; Calbiochem) was suspended in vehicle (40% polyethylene glycol 1000, 10% povidone C30 and 2% benzyl alcohol in distilled water) and injected intraperitoneally (10 mg/kg). siEphA2 (Eurogentec; 7.5 μg/mouse) was delivered using *in vivo* jetPEI® according to the manufacturer's instructions (Polyplus transfection) and injected subcutaneously near the tumor mass. Tumor volume was determined throughout the experiment by measuring the length (l) and width (w) and then calculated as $\pi/6 \times l \times w \times (l+w)/2$.

For analyses of breast cancer cell dissemination in mice, xenograft experiments were conducted using MDA-MB-231 HA-TrkA cells. The tumors were allowed to

develop for 14 days and the mice were then submitted to 5 injections (every 3 days) of either scrambled siRNA, or TrkA- and EphA2-targeting siRNAs alone or in combination (7.5 µg siRNA/mouse). Tumor volume was determined throughout the experiment by measuring the length (l) and width (w) and tumors were allowed to grow up to 2 cm^3 to allow metastasis of cancer cells. After animal sacrifice, lungs, liver and brain were collected and detection of cancer cells in those organs was carried out by evaluating human microglobulin mRNA expression by RT-PCR as previously described [17].

2.8. Statistical analysis

Results are expressed as mean ± SEM of at least three independent experiments. Two-tailed unpaired Student t-tests, one-way or two-way ANOVA tests (Bonferroni's post-hoc test) and Mann-Whitney tests were used where appropriate.

3. Results

3.1. TrkA is associated with sortilin and EphA2 in proNGF-treated MDA-MB-231 breast cancer cells

In order to decipher TrkA signaling partners under proNGF stimulation, we first performed proteomic analysis in MDA-MB-231 breast cancer cells stably expressing HA-tagged TrkA [10]. Proteins co-immunoprecipitated with HA-TrkA were identified by mass spectrometry analysis (Figure 1). Individual proteins (985) were identified in selected bands from cells treated with proNGF (5 and 30 min) (Figure 1A). Using Panther classification software, we observed that most of the identified proteins were implicated in maturation and vesicular trafficking (binding and catalytic activities). Seven percent were related to membrane receptor and signaling (Figure 1B). As expected, sortilin, the known receptor of proNGF was found to be co-immunoprecipitated with HA-TrkA (Figure 1C). Interestingly, we found that EphA2, a membrane receptor tyrosine kinase, was also co-immunoprecipitated with HA-TrkA. EphA2 is of particular interest, as it is known to be expressed in breast cancer in which it favors aggressive behavior and metastases formation [18]. We also identified Src, cortactin and p130 Cas (BCAR1, *Breast cancer anti-estrogen resistance protein 1*), which are reported to act as early effectors in EphA2 downstream signaling pathways [19]. Other proteins such as SHEP1 (SH2D3C, *SH2 domain-containing protein 3C*), PTP-PEST (PTPN12, *Tyrosine-protein phosphatase non-receptor type 12*) and RIL (PDLI4, *PDZ and LIM domain protein 4*) were also found to be pulled-down with TrkA; these proteins are well known to regulate Src and/or p130 Cas-mediated signaling pathways [20–22]. The other identified proteins including Lasp1 (*LIM and SH3 domain protein 1)*, SNAP23 (*Synaptosomal-associated protein 23),* FHL2 (*Four and a half LIM domains protein 2*), HAX1 (*HCLS1-associated protein X-1)*, adducin, MARCKS (*Myristoylated*

243 *alanine-rich C-kinase substrate)* gelsolin, and integrins $\alpha_3\beta_1$ are downstream targets
244 of Src and p130 Cas, which are associated with cytoskeleton remodeling and cell
245 migration [23–28].
246 To confirm proNGF-induced TrkA association with sortilin and EphA2 in breast
247 cancer cells, we further performed immunoprecipitation assays by using antibodies
248 against HA (-TrkA), sortilin and EphA2, followed by Western blot analysis (Figure
249 2A). In the absence of proNGF, none of the three receptors was found to be co-
250 immunoprecipitated. Upon proNGF treatment, sortilin and EphA2 were co-
251 immunoprecipitated with TrkA. These results were confirmed by reverse co-
252 immunoprecipitation of sortilin and EphA2 (Figure 2A). Of note, in the presence of
253 NGF, sortilin binding to TrkA was detected after 30 min of treatment but EphA2
254 binding was not observed after neither 5 min nor 30 min of treatment (Figure 2A).
255 Thus, NGF seemed to induce a late TrkA/sortilin association, suggesting that sortilin
256 acts as an endocytic receptor, as previously reported in neuronal cell models [8].
257 Proximity ligation assays (PLA) were then carried out to confirm any receptor
258 association (distance <40 nm) at the plasma membrane. In the absence of
259 exogenous proNGF stimulation, a basal PLA signal (red dots) was observed for
260 sortilin/TrkA (Figure 2B-C) and TrkA/EphA2 (Figure 2D-E). ProNGF stimulation (5
261 min) enhanced PLA signals of sortilin/TrkA and EphA2/TrkA (Figure 2C and 2E);
262 this increase was transient as membrane PLA signals decreased to basal levels
263 after 30 min of proNGF treatment.
264 Together, these data indicated that proNGF specifically induces the association of
265 TrkA with sortilin and EphA2, even if we cannot exclude the existence of other
266 intermediary partners.

3.2. Sequential sortilin/TrkA/EphA2 association induces TrkA-dependent Akt phosphorylation and EphA2-dependent Src phosphorylation

In order to put insight into the dynamics of the receptors association, we first treated cells with neurotensin that inhibits, by competition, proNGF binding to sortilin [8]. As shown in Figure 3A, in the presence of neurotensin, TrkA was not immunoprecipitated with either sortilin or EphA2, indicating that proNGF binding to sortilin was necessary for sortilin/TrkA/EphA2 association. When TrkA expression was silenced by siRNA (Figure 3B, S1), sortilin did not pull-down EphA2, indicating that sortilin could not associate with EphA2 in the absence of TrkA; this was further confirmed by PLA, as no signal was detected for sortilin/EphA2.

Interestingly, in cells stably expressing a kinase-dead TrkA that prevents receptor phosphorylation (Figure 3D), proNGF still induced TrkA association with sortilin and EphA2, suggesting that TrkA phosphorylation was not necessary for sortilin/TrkA/EphA2 association. Finally, when EphA2 expression was silenced by siRNA (Figure 3E), TrkA and sortilin were co-immunoprecipitated in proNGF-treated cells, indicating that EphA2 was not required for TrkA and sortilin association.

Together, these results suggested that proNGF binding to sortilin elicits sortilin association with TrkA, which in turn recruits EphA2 at cell surface.

As we have previously shown that proNGF stimulates breast cancer cell invasion through TrkA activation, we asked if EphA2 could be involved in TrkA-mediated cell invasion. When EphA2 expression was inhibited by siRNA approach, proNGF was no longer able to stimulate cell invasion both in native and HA-TrkA over-expressing MDA-MB-231 cells (Figure S2), implying that EphA2 was necessary for proNGF-stimulated and TrkA-mediated cell invasion. ProNGF-stimulated invasion implicates the activation of downstream signaling pathways including Akt and Src [10]. On the

other hand, Src is also a downstream effector of EphA2 [19], we then determined the respective role of TrkA and EphA2 in Akt and Src activation by using a kinase-dead mutant of TrkA (Figure 3F) or siEphA2 approach (Figure 3G). Following proNGF treatment, Akt was not phosphorylated in cells expressing a kinase-dead mutant of TrkA while Src phosphorylation was maintained (Figure 3F), indicating that Akt phosphorylation depended upon TrkA phosphorylation while Src phosphorylation did not. By contrary, in cells transfected with siEphA2, proNGF still induced Akt phosphorylation but not that of Src, indicating that Akt phosphorylation did not depend on EphA2 while Src activation did (Figure 3G).

Collectively, our data showed that, in MDA-MB-231 breast cancer cells, proNGF binding to sortilin induced functional sortilin/TrkA/EphA2 association, leading to TrkA-dependent Akt phosphorylation and EphA2-dependent Src phosphorylation (Figure 3H).

3.3. ProNGF increases breast cell clonogenic growth through functional association of TrkA with EphA2

In order to determine the relevance of TrkA/EphA2 functional association in breast cancer cells, we further extended our study on a panel of representative breast cancer cell lines including basal-like (wild type MDA-MB-231, SUM159-PT), luminal-like (MCF-7, T-47D), and HER2-overexpressing basal-like cell line HCC-1954. PLA signals of TrkA/EphA2 were increased after 5 min of stimulation with proNGF in all cell lines tested, except for MCF-7 (Figures 4A and S3). Clonogenic assays were then carried out to evaluate the impact of EphA2 invalidation on proNGF-stimulated cell growth. As shown in Figure 4B, proNGF stimulated clonogenic cell growth in all the cell lines tested; siEphA2 totally abolished proNGF-induced cell growth except in MCF-7, this was consistent with the results of PLA assay revealing that proNGF

318 did not increase TrkA/EphA2 complex in these cells and with the fact that MCF-7
319 cells express low levels of both TrkA and EphA2 compared to the other cell lines
320 (Figure S4). Use of another siEphA2 sequence [14] confirmed also the implication
321 of EphA2 in pro-NGF induced clonogenic growth of MDA-MB-231 cells (Figure S5).
322 These results indicated that proNGF-induced cell growth involved TrkA/EphA2
323 association in different cell lines whatever their molecular classification (*i.e.* basal,
324 luminal or HER2-like). We then examined the impact of TrkA and/or EphA2 inhibition
325 on colony formation in MDA-MB-231 cells. As shown in Figure 4C, the TrkA inhibitor
326 K252a inhibited colony formation to about 85 % of control, siEphA2 to 60 % of
327 control, while combinatory treatment with K252a and siEphA2 inhibited colony
328 formation to less than 30 % of control.
329
330 3.4 Simultaneous targeting of TrkA and EphA2 reduces tumor growth and brain
331 metastasis *in vivo*
332 Given the above results indicating the importance of proNGF-induced TrkA/EphA2
333 association in breast cancer cells, we determined the potential benefit of a
334 combinatorial targeting of TrkA and EphA2 in xenograft mouse model. As shown in
335 Figure 5A and B, CEP-701 (clinical derivative of K252a) alone did not significantly
336 reduce tumor growth, while siEphA2 alone delayed tumor growth when compared
337 to the control group (scrambled siRNA). Combined treatment of CEP-701 and
338 siEphA2 resulted in a dramatic reduction of tumor burden when compared to CEP-
339 701 or siEphA2 treatment alone. We then evaluated the impact of TrkA and/or
340 EphA2 invalidation on breast cancer cell dissemination in different organs including
341 lungs, liver and brain (Figure 5C). In these conditions, we first confirmed that
342 combined inhibition of TrkA and EphA2 inhibited tumor growth as the median

343 survival of the mice was increased: Median of survival were 40 days in control group,
344 53 days in siTrkA group, 49 days in siEphA2 group and 57.5 days in siTrkA and
345 siEphA2 mice (Figure S6). We found that tumor cells disseminated readily in these
346 three distant organs. Lung metastasis was not modified under any invalidation
347 condition. Interestingly, TrkA invalidation alone was sufficient to reduce liver
348 metastasis while combined inhibition of TrkA and EphA2 was required to decrease
349 brain metastasis. These results indicated that simultaneous inhibition of TrkA and
350 EphA2 was not only efficient in inhibiting primary tumor growth, but also in reducing
351 brain metastasis formation.

352

353 3.5. ProNGF-induced TrkA/EphA2 association is correlated with poor prognosis in
354 breast cancer

355 To go further on the significance of TrkA/EphA2 functional complex in breast cancer,
356 we performed immunostainings of TrkA, EphA2, and PLA labeling to colocalize
357 TrkA/EphA2 in breast tumor samples in a tissue microarray (TMA) cohort of 189
358 patients (Figure 6, Table 1 and S1). We found that TrkA expression was associated
359 with PR-negative status (Table 1). However, neither TrkA nor EphA2 alone
360 correlated with overall survival of patients (Figure 6A-H and Table 1). By PLA, we
361 distinguished the differential PLA signals of TrkA/EphA2 in the samples, and found
362 that high level of TrkA/EphA2 PLA signals in tumors was correlated with a significant
363 decrease of overall survival of patients (Figure 6I-L).

364

4. Discussion

Compelling evidences showed that proNGF is more than just a metabolic precursor of NGF, as it exhibits biological activities in a wide range of normal and neoplastic tissues, including breast cancer [6,8–13,17]. Nevertheless, proNGF functions in cells are still in debate due to its pro-survival and pro-apoptotic activities, according to cell types. A recent study reconciled these findings by showing that these opposite biological effects depend on TrkA levels [29]. Indeed, the authors showed that proNGF elicits apoptotic signaling in PC-12 cells expressing low levels of TrkA while it favors survival of cells expressing high levels of TrkA. In agreement with these findings, increased levels of TrkA are associated with tumor growth and metastasis in breast cancer [30] and melanoma [31].

In breast cancer cells, we previously observed that uncleavable proNGF induces sortilin recruitment at plasma membrane and TrkA activation, leading to increased cell invasion, independently of $p75^{NTR}$ [10]. Herein, by studying TrkA-interacting proteins upon proNGF stimulation, we identified EphA2, a membrane receptor tyrosine kinase, as a key element of proNGF signaling in breast cancer cells. ProNGF signaling through sortilin and TrkA allowed for EphA2 recruitment, which in turn activated Src in a TrkA phosphorylation-independent manner.

Implications of EphA2 in proNGF-induced signaling is of particular interest. Indeed, EphA2 binds to its ligand ephrin-A1 to maintain cell adhesion and tissue homeostasis in normal breast epithelial cells [32], ephrin-A1 downregulation favors ligand-independent activation of EphA2 and associated downstream signaling pathways (*e.g.* MAP-kinase, RhoGTPase and Src) in several types of cancer cells, leading to cell invasion and metastasis [33–35]. Although the mechanisms of ligand-independent activation of EphA2 remain fragmentary, it has been shown that EphA2

390 phosphorylation by Akt or Rsk can lead to its activation [35,36]. Here, we observed
391 that in the context of proNGF stimulation, EphA2 activated Src *via* an Akt-
392 phosphorylation independent mechanism. Moreover, our proteomic analysis
393 revealed that several Src-associated signaling proteins like cortactin and p130 Cas
394 were pulled-down with TrkA upon proNGF treatment, suggesting that proNGF could
395 activate a signaling cascade involving Src/p130 Cas/cortactin complex. Although
396 further study should be done to confirm this hypothesis, the Src/p130 Cas/cortactin
397 complex is already reported to induce cell invasion [37].
398 Song *et al.* [14] have recently reported that EphA2 is overexpressed in the basal-
399 like breast cancer molecular subtype and this overexpression is correlated with poor
400 recurrence-free survival in triple-negative breast cancers. Loss of EphA2 function in
401 both human and genetically engineered mouse models of triple negative breast
402 cancers reduced tumor growth. Herein, we observed that EphA2 silencing inhibited
403 proNGF-stimulated clonogenic cell growth of not only triple negative, but also
404 luminal ER-positive and HER2-positive breast cancer cell lines. This implies that
405 EphA2 is involved in proNGF-stimulated clonogenic cell growth, independently of
406 molecular subtypes. Consistently, we could not find any significant correlation
407 between TrkA/EphA2 complex or co-localization and different subtypes of breast
408 cancer. Of importance, the level of TrkA/EphA2 co-localization is significantly
409 correlated with poor overall survival of patients suffering from breast cancer
410 regardless the cancer subtype, suggesting the potential involvement of
411 proNGF/TrkA/EphA2 axis in breast cancer progression whatever the cancer
412 subtype. These findings reinforced our previous results showing a significant
413 correlation between the expression of proNGF and lymph node invasion [10].

Cross-talk in growth factor-induced signaling pathway is a leading cause of resistance to targeted therapies [38,39]. EphA2 was identified to mediate resistance to multiple targeted therapies including trastuzumab (HER-2 inhibitor) *via* Src activation in breast cancer cells [40], as well as erlotinib (EGFR inhibitor) in lung cancer models [41]. We postulate that the existence of a proNGF-induced EphA2-Src pathway, independently of TrkA phosphorylation and Akt activation, may contribute to tumor resistance to therapies targeting TrkA kinase domain (lestaurtinib, larotrectinib, entrectinib…). Here, we showed that simultaneous targeting of TrkA and EphA2 receptors, dramatically reduced colony formation *in vitro* and tumor development *in vivo*, suggesting that inhibiting both TrkA- and EphA2-dependent signaling pathways may improve the therapeutic benefit in patients (over)expressing TrkA, EphA2 and proNGF.

In conclusion, our data demonstrated that functional interactions between sortilin, TrkA and EphA2 are essential for the tumor-promoting effect of proNGF in breast cancer. Although further translational work is required, our results suggest that proNGF/TrkA/EphA2 axis could be used as both a prognostic marker and a potential therapeutic target in breast cancer.

Acknowledgments

We thank Anne-Sophie Lacoste who performed the mass spectrometry analysis (Mass Spectrometry facility, IFR-147, University Lille, France). We also thank the animal facility at the Pasteur Institute of Lille (PLETHA) for animal housing (Dr J.P. de Cavel, M T Chassat).

Conflicts of interest

All authors declare no conflict of interest

Reference

[1] T.R. Wilson, J. Fridlyand, Y. Yan, E. Penuel, L. Burton, E. Chan, J. Peng, E. Lin, Y. Wang, J. Sosman, A. Ribas, J. Li, J. Moffat, D.P. Sutherlin, H. Koeppen, M. Merchant, R. Neve, J. Settleman, Widespread potential for growth-factor-driven resistance to anticancer kinase inhibitors, Nature. 487 (2012) 505–509. doi:10.1038/nature11249.

[2] S. Gusenbauer, P. Vlaicu, A. Ullrich, HGF induces novel EGFR functions involved in resistance formation to tyrosine kinase inhibitors, Oncogene. 32 (2013) 3846–3856. doi:10.1038/onc.2012.396.

[3] B.L. Hempstead, D. Martin-Zanca, D.R. Kaplan, L.F. Parada, M.V. Chao, High-affinity NGF binding requires coexpression of the trk proto-oncogene and the low-affinity NGF receptor, Nature. 350 (1991) 678–683. doi:10.1038/350678a0.

[4] B.A. Tsui-Pierchala, J. Milbrandt, E.M. Johnson, NGF utilizes c-Ret via a novel GFL-independent, inter-RTK signaling mechanism to maintain the trophic status of mature sympathetic neurons, Neuron. 33 (2002) 261–273.

[5] C. Festuccia, G.L. Gravina, P. Muzi, D. Millimaggi, V. Dolo, C. Vicentini, C. Ficorella, E. Ricevuto, M. Bologna, Her2 crosstalks with TrkA in a subset of prostate cancer cells: rationale for a guided dual treatment, Prostate. 69 (2009) 337–345. doi:10.1002/pros.20884.

[6] O. Clewes, M.S. Fahey, S.J. Tyler, J.J. Watson, H. Seok, C. Catania, K. Cho, D. Dawbarn, S.J. Allen, Human ProNGF: biological effects and binding profiles at TrkA, P75NTR and sortilin, J. Neurochem. 107 (2008) 1124–1135. doi:10.1111/j.1471-4159.2008.05698.x.

[7] D. Feng, T. Kim, E. Ozkan, M. Light, R. Torkin, K.K. Teng, B.L. Hempstead, K.C. Garcia, Molecular and structural insight into proNGF engagement of p75NTR and sortilin, J. Mol. Biol. 396 (2010) 967–984. doi:10.1016/j.jmb.2009.12.030.

[8] A. Nykjaer, R. Lee, K.K. Teng, P. Jansen, P. Madsen, M.S. Nielsen, C. Jacobsen, M. Kliemannel, E. Schwarz, T.E. Willnow, B.L. Hempstead, C.M. Petersen, Sortilin is essential for proNGF-induced neuronal cell death, Nature. 427 (2004) 843–848. doi:10.1038/nature02319.

[9] R. Masoudi, M.S. Ioannou, M.D. Coughlin, P. Pagadala, K.E. Neet, O. Clewes, S.J. Allen, D. Dawbarn, M. Fahnestock, Biological activity of nerve growth factor precursor is dependent upon relative levels of its receptors, J. Biol. Chem. 284 (2009) 18424–18433. doi:10.1074/jbc.M109.007104.

[10] Y. Demont, C. Corbet, A. Page, Y. Ataman-Önal, G. Choquet-Kastylevsky, I. Fliniaux, X. Le Bourhis, R.-A. Toillon, R.A. Bradshaw, H. Hondermarck, Pro-nerve growth factor induces autocrine stimulation of breast cancer cell invasion through tropomyosin-related kinase A (TrkA) and sortilin protein, J. Biol. Chem. 287 (2012) 1923–1931. doi:10.1074/jbc.M110.211714.

[11] J. Pundavela, Y. Demont, P. Jobling, L.F. Lincz, S. Roselli, R.F. Thorne, D. Bond, R.A. Bradshaw, M.M. Walker, H. Hondermarck, ProNGF correlates with Gleason score and is a potential driver of nerve infiltration in prostate cancer, Am. J. Pathol. 184 (2014) 3156–3162. doi:10.1016/j.ajpath.2014.08.009.

[12] F. Truzzi, A. Marconi, R. Lotti, K. Dallaglio, L.E. French, B.L. Hempstead, C. Pincelli, Neurotrophins and their receptors stimulate melanoma cell proliferation and migration, J. Invest. Dermatol. 128 (2008) 2031–2040. doi:10.1038/jid.2008.21.

[13] S. Faulkner, S. Roselli, Y. Demont, J. Pundavela, G. Choquet, P. Leissner, C. Oldmeadow, J. Attia, M.M. Walker, H. Hondermarck, ProNGF is a potential

diagnostic biomarker for thyroid cancer, Oncotarget. 7 (2016) 28488–28497. doi:10.18632/oncotarget.8652.
[14] W. Song, Y. Hwang, V.M. Youngblood, R.S. Cook, J.M. Balko, J. Chen, D.M. Brantley-Sieders, Targeting EphA2 impairs cell cycle progression and growth of basal-like/triple-negative breast cancers, Oncogene. 36 (2017) 5620–5630. doi:10.1038/onc.2017.170.
[15] L. Aubert, M. Guilbert, C. Corbet, E. Génot, E. Adriaenssens, T. Chassat, F. Bertucci, T. Daubon, N. Magné, X.L. Bourhis, R.-A. Toillon, NGF-induced TrkA/CD44 association is involved in tumor aggressiveness and resistance to lestaurtinib, Oncotarget. 6 (2015) 9807–9819. doi:10.18632/oncotarget.3227.
[16] R.-A. Toillon, C. Lagadec, A. Page, V. Chopin, P.-E. Sautière, J.-M. Ricort, J. Lemoine, M. Zhang, H. Hondermarck, X. Le Bourhis, Proteomics demonstration that normal breast epithelial cells can induce apoptosis of breast cancer cells through insulin-like growth factor-binding protein-3 and maspin, Mol. Cell Proteomics. 6 (2007) 1239–1247. doi:10.1074/mcp.M600477-MCP200.
[17] E. Tomellini, Y. Touil, C. Lagadec, S. Julien, P. Ostyn, N. Ziental-Gelus, S. Meignan, J. Lengrand, E. Adriaenssens, R. Polakowska, X. Le Bourhis, Nerve growth factor and proNGF simultaneously promote symmetric self-renewal, quiescence, and epithelial to mesenchymal transition to enlarge the breast cancer stem cell compartment, Stem Cells. 33 (2015) 342–353. doi:10.1002/stem.1849.
[18] D.P. Zelinski, N.D. Zantek, J.C. Stewart, A.R. Irizarry, M.S. Kinch, EphA2 overexpression causes tumorigenesis of mammary epithelial cells, Cancer Res. 61 (2001) 2301–2306.
[19] L. Faoro, P.A. Singleton, G.M. Cervantes, F.E. Lennon, N.W. Choong, R. Kanteti, B.D. Ferguson, A.N. Husain, M.S. Tretiakova, N. Ramnath, E.E. Vokes, R. Salgia, EphA2 mutation in lung squamous cell carcinoma promotes increased cell survival, cell invasion, focal adhesions, and mammalian target of rapamycin activation, J. Biol. Chem. 285 (2010) 18575–18585. doi:10.1074/jbc.M109.075085.
[20] M.A. Chellaiah, M.D. Schaller, Activation of Src kinase by protein-tyrosine phosphatase-PEST in osteoclasts: comparative analysis of the effects of bisphosphonate and protein-tyrosine phosphatase inhibitor on Src activation in vitro, J. Cell. Physiol. 220 (2009) 382–393. doi:10.1002/jcp.21777.
[21] S. Roselli, Y. Wallez, L. Wang, V. Vervoort, E.B. Pasquale, The SH2 domain protein Shep1 regulates the in vivo signaling function of the scaffolding protein Cas, Cell. Signal. 22 (2010) 1745–1752. doi:10.1016/j.cellsig.2010.06.015.
[22] Y. Zhang, Y. Tu, J. Zhao, K. Chen, C. Wu, Reversion-induced LIM interaction with Src reveals a novel Src inactivation cycle, J. Cell Biol. 184 (2009) 785–792. doi:10.1083/jcb.200810155.
[23] B. Fadeel, E. Grzybowska, HAX-1: a multifunctional protein with emerging roles in human disease, Biochim. Biophys. Acta. 1790 (2009) 1139–1148. doi:10.1016/j.bbagen.2009.06.004.
[24] T.G.P. Grunewald, U. Kammerer, E. Schulze, D. Schindler, A. Honig, M. Zimmer, E. Butt, Silencing of LASP-1 influences zyxin localization, inhibits proliferation and reduces migration in breast cancer cells, Exp. Cell Res. 312 (2006) 974–982. doi:10.1016/j.yexcr.2005.12.016.
[25] M.J. Kean, K.C. Williams, M. Skalski, D. Myers, A. Burtnik, D. Foster, M.G. Coppolino, VAMP3, syntaxin-13 and SNAP23 are involved in secretion of

matrix metalloproteinases, degradation of the extracellular matrix and cell invasion, J. Cell. Sci. 122 (2009) 4089–4098. doi:10.1242/jcs.052761.
[26] Y. Matsuoka, X. Li, V. Bennett, Adducin: structure, function and regulation, Cell. Mol. Life Sci. 57 (2000) 884–895. doi:10.1007/PL00000731.
[27] K. Mitchell, K.B. Svenson, W.M. Longmate, K. Gkirtzimanaki, R. Sadej, X. Wang, J. Zhao, A.G. Eliopoulos, F. Berditchevski, C.M. Dipersio, Suppression of integrin alpha3beta1 in breast cancer cells reduces cyclooxygenase-2 gene expression and inhibits tumorigenesis, invasion, and cross-talk to endothelial cells, Cancer Res. 70 (2010) 6359–6367. doi:10.1158/0008-5472.CAN-09-4283.
[28] W. Zhang, B. Jiang, Z. Guo, C. Sardet, B. Zou, C.S.C. Lam, J. Li, M. He, H.-Y. Lan, R. Pang, I.F.N. Hung, V.P.Y. Tan, J. Wang, B.C.Y. Wong, Four-and-a-half LIM protein 2 promotes invasive potential and epithelial-mesenchymal transition in colon cancer, Carcinogenesis. 31 (2010) 1220–1229. doi:10.1093/carcin/bgq094.
[29] M.S. Ioannou, M. Fahnestock, ProNGF, but Not NGF, Switches from Neurotrophic to Apoptotic Activity in Response to Reductions in TrkA Receptor Levels, Int J Mol Sci. 18 (2017). doi:10.3390/ijms18030599.
[30] B. Davidson, R. Reich, P. Lazarovici, V. Ann Flørenes, S. Nielsen, J.M. Nesland, Altered expression and activation of the nerve growth factor receptors TrkA and p75 provide the first evidence of tumor progression to effusion in breast carcinoma, Breast Cancer Res. Treat. 83 (2004) 119–128. doi:10.1023/B:BREA.0000010704.17479.8a.
[31] O. Shonukan, I. Bagayogo, P. McCrea, M. Chao, B. Hempstead, Neurotrophin-induced melanoma cell migration is mediated through the actin-bundling protein fascin, Oncogene. 22 (2003) 3616–3623. doi:10.1038/sj.onc.1206561.
[32] E.B. Pasquale, Eph-ephrin bidirectional signaling in physiology and disease, Cell. 133 (2008) 38–52. doi:10.1016/j.cell.2008.03.011.
[33] W.B. Fang, R.C. Ireton, G. Zhuang, T. Takahashi, A. Reynolds, J. Chen, Overexpression of EPHA2 receptor destabilizes adherens junctions via a RhoA-dependent mechanism, J. Cell. Sci. 121 (2008) 358–368. doi:10.1242/jcs.017145.
[34] N. Hiramoto-Yamaki, S. Takeuchi, S. Ueda, K. Harada, S. Fujimoto, M. Negishi, H. Katoh, Ephexin4 and EphA2 mediate cell migration through a RhoG-dependent mechanism, J. Cell Biol. 190 (2010) 461–477. doi:10.1083/jcb.201005141.
[35] H. Miao, D.-Q. Li, A. Mukherjee, H. Guo, A. Petty, J. Cutter, J.P. Basilion, J. Sedor, J. Wu, D. Danielpour, A.E. Sloan, M.L. Cohen, B. Wang, EphA2 mediates ligand-dependent inhibition and ligand-independent promotion of cell migration and invasion via a reciprocal regulatory loop with Akt, Cancer Cell. 16 (2009) 9–20. doi:10.1016/j.ccr.2009.04.009.
[36] Y. Zhou, N. Yamada, T. Tanaka, T. Hori, S. Yokoyama, Y. Hayakawa, S. Yano, J. Fukuoka, K. Koizumi, I. Saiki, H. Sakurai, Crucial roles of RSK in cell motility by catalysing serine phosphorylation of EphA2, Nat Commun. 6 (2015) 7679. doi:10.1038/ncomms8679.
[37] S.M. MacGrath, A.J. Koleske, Cortactin in cell migration and cancer at a glance, J Cell Sci. 125 (2012) 1621–1626. doi:10.1242/jcs.093781.
[38] K. Berns, R. Bernards, Understanding resistance to targeted cancer drugs through loss of function genetic screens, Drug Resist. Updat. 15 (2012) 268–275. doi:10.1016/j.drup.2012.10.002.

[39] J.M. Stommel, A.C. Kimmelman, H. Ying, R. Nabioullin, A.H. Ponugoti, R. Wiedemeyer, A.H. Stegh, J.E. Bradner, K.L. Ligon, C. Brennan, L. Chin, R.A. DePinho, Coactivation of receptor tyrosine kinases affects the response of tumor cells to targeted therapies, Science. 318 (2007) 287–290. doi:10.1126/science.1142946.

[40] G. Zhuang, D.M. Brantley-Sieders, D. Vaught, J. Yu, L. Xie, S. Wells, D. Jackson, R. Muraoka-Cook, C. Arteaga, J. Chen, Elevation of receptor tyrosine kinase EphA2 mediates resistance to trastuzumab therapy, Cancer Res. 70 (2010) 299–308. doi:10.1158/0008-5472.CAN-09-1845.

[41] K.R. Amato, S. Wang, L. Tan, A.K. Hastings, W. Song, C.M. Lovly, C.B. Meador, F. Ye, P. Lu, J.M. Balko, D.C. Colvin, J.M. Cates, W. Pao, N.S. Gray, J. Chen, EPHA2 Blockade Overcomes Acquired Resistance to EGFR Kinase Inhibitors in Lung Cancer, Cancer Res. 76 (2016) 305–318. doi:10.1158/0008-5472.CAN-15-0717.

606 **TABLE**

607

608 **Table 1:** Correlation between expression levels of TrkA and EphA2, TrkA/EphA2
609 association (PLA signal) and clinical parameters of patient samples

610

		TrkA	EphA2	TrkA/EphA2 PLA
Estrogen receptor	**Positive (n=109)**	1.725±0.09478 p= 0.1408	1.817±0.1011 p=0.2155	2.193±0.1169 p=0.1608
	Negative (n=71)	1.944±0.1115	2.014±0.1212	1.915±0.1615
Progesterone receptor	**Positive (n=95)**	**1.663±0.09996 p=0.0318**	1.758±0.1097 p=0.0536	2.053±0.1201 p=0.5557
	Negative (n=84)	**1.976±0.1044**	2.060±0.1089	2.141±0.1541
HER-2	**Positive (n=69)**	1.783±0.1254 p=0.8799	1.884±0.1248 p=0.9606	2.217±0.1650 p=0.2717
	Negative (n=113)	1.805±0.08876	1.876±0.09988	2.000±0.1166
Triple negative	**Positive (n=34)**	2.088±0.1544 p=0.0578	2.176±0.1661 p=0.0715	1.765±0.2315 p=0.1053
	Negative (n=147)	1.735±0.08153	1.816±0.08743	2.163±0.1049
Lymph node invasion	**Positive (n=116)**	1.724±0.09372 p=0.1166	1.897±0.09976 p=0.9171	2.138±0.1193 p=0.2127
	Negative (n=69)	1.957±0.1081	1.913±0.1181	1.899±0.1193

611

FIGURE LEGENDS

Figure 1: Proteomic analysis of HA-TrkA partners revealed EphA2 association and downstream signaling pathways proteins. (A) MDA-MB-231 HA-TrkA cells were treated in absence or presence of non-cleavable proNGF (0.5nM) for 5 and 30 min. Total cell lysates were subjected to HA immunoprecipitation and separated in 10% SDS-PAGE. Proteins were revealed by colloidal blue Coomassie staining. Using transilluminator, intensity of bands was appreciated by CC and R-A T and bands with stronger intensity than that of control were cut (red square). Protein peptide digests were then subjected to mass spectrometry analysis. **(B)** Identified proteins were analyzed for Biological pathways using Panther software. **(C)** Mass spectrometry identification of selected putative interacting partners of TrkA under proNGF stimulation (5 or 30 min). For each identified protein, the Uniprot ID, the number and sequence of the different peptides allowing protein identification and the individual peptide Mascot score are summarized. Underlined amino-acids (C and M) are oxidized residues. MW: Molecular Weight. GO: Gene Ontology.

Figure 2: ProNGF induced association of sortilin, TrkA and EphA2. (A) Representative immunoblotting for sortilin, EphA2 and TrkA following IP anti-HA (TrkA), sortilin or EphA2 in HA-TrkA MDA-MB-231 cells after non-cleavable proNGF treatment. **(B-E)** Representative pictures (B and D) and quantification (C and E) for sortilin/TrkA (B and C) and TrkA/EphA2 (D and E) PLA signals in HA-TrkA MDA-MB-231 cells after non-cleavable proNGF treatment. PLA signals were quantified on three independent experiments. In (C) and (E), data are expressed as scatter plots. ***p<0.001; ns, not significant.

Figure 3: ProNGF-induced association of TrkA with sortilin and EphA2 was sequential.

(A-B) Representative immunoblotting for sortilin, EphA2 and TrkA after IP anti-HA (TrkA) following treatment with 1 µM neurotensin (A) or after IP anti-sortilin in cells transfected with TrkA-targeting siRNA (B). **(C)** Representative pictures of sortilin/EphA2 PLA. **(D-E)** Representative immunoblotting for sortilin, EphA2 and TrkA after IP anti-HA in HA-TrkA MDA-MB-231 cells expressing a kinase-dead TrkA mutant (D) or transfected with EphA2-targeting siRNA (E). In (D), TrkA phosphorylation in the kinase domain (Y674/675 residues) was also evaluated by immunoblotting. **(F-G)** Representative immunoblotting for the phosphorylated and total forms of Akt and Src in non-cleavable proNGF-stimulated HA-TrkA MDA-MB-231 cells expressing a kinase-dead TrkA mutant (F) or cells transfected with EphA2-targeting siRNA (G). Immunoprecipitations and immunoblots were carried out at least 2 times with similar results. **(H)** Putative dynamic of proNGF-induced sortilin/TrkA/EphA2 signaling in breast cancer cells. After proNGF binding to sortilin (1), TrkA is phosphorylated allowing Akt activation (2). Additionally, EphA2 is also recruited to the sortilin/TrkA complex in a TrkA kinase-independent manner, leading to Src activation (3).

Figure 4: TrkA/EphA2 complex was involved in proNGF-stimulated clonogenic cell growth. (A) PLA of TrkA/EphA2 complex in wild-type MDA-MB-231, SUM159-PT, MCF-7, T-47D and HCC-1954 breast cancer cells following proNGF treatment (5 and 30 min). **(B)** Clonogenic cell growth following proNGF treatment (5 and 30 min) and transfection of EphA2-targeting siRNA. **(C)** Clonogenic cell growth of MDA-MB-231 cells following treatment with 10 nM K252a and/or transfection with EphA2-

targeting siRNA. Data are expressed as scatter plots (A) or means ± SEM (B-C). **p<0.01; ***p<0.001; ns, not significant.

Figure 5: Combinatorial treatment with TrkA- and EphA2-targeting modalities delays primary tumor growth and metastasis formation. **(A-B)** Tumor growth of MDA-MB-231 xenografts in SCID mice submitted to 3 injections (every 3 days; black arrows) of either *in vivo* JetPEI + control or EphA2-targeting siRNA (7.5 µg/mouse), or CEP-701 (10 mg/kg) alone or in combination. Tumor volumes were measured at different intervals (A) and represented as scatter plots at the end of the experiment (B). (**C**) Detection of metastatic human breast cancer cells (as determined by RT-PCR for the expression of the human microglobulin) in different organs (lungs, liver and brain) of MDA-MB-231 xenograft-bearing mice submitted to 5 injections (every 3 days; black arrows) of either *in vivo* JetPEI + control or EphA2-targeting siRNA (7.5 µg/mouse), or CEP-701 (10 mg/kg) alone or in combination. *p<0.05; **p<0.01; ***p<0.001; ns: not significant. Data are expressed as means ± SEM (A) or scatter plots (B).

Figure 6: TrkA/EphA2 complex expression is associated with overall survival (OS) decrease for breast cancer patients. (A-C) Representative pictures for TrkA immunostaining in breast tumors, defined as low (A), medium (B) or high (C). **(D)** Kaplan-Meier OS curves in breast cancer patients according to TrkA staining. **(E-G)** Representative pictures for EphA2 immunostaining in breast tumors, defined as low (E), medium (F) or high (G). **(H)** Kaplan-Meier OS curves in breast cancer patients according to EphA2 staining. **(I-K)** Representative PLA images depicting low (I), medium (J) and high staining (K) for TrkA/EphA2 complex on patient breast tumor

688 samples. **(L)** Kaplan-Meier OS curves in breast cancer patients according to
689 TrkA/EphA2 complex abundance.

A

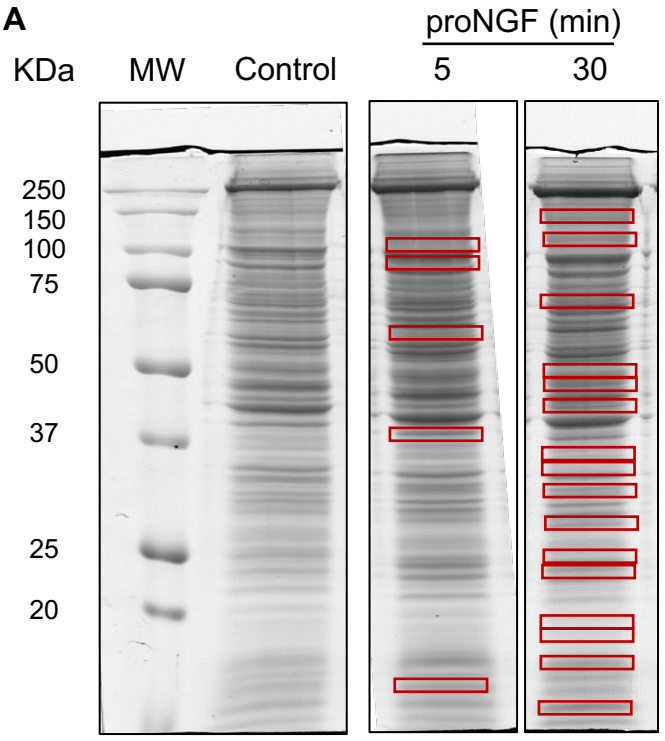

B

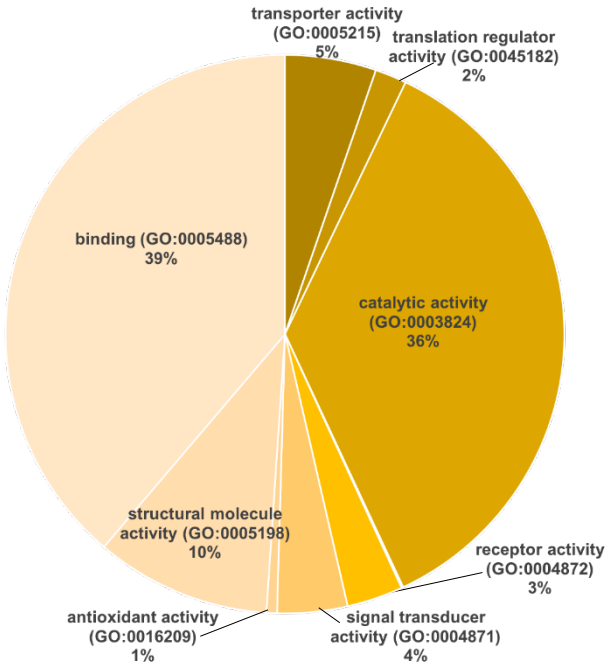

C

Protein name	Uniprot ID	Peptide sequences	Mascot score
Sortilin	Q99523	IYSFGLGGR	31
EphA2	P29317	FADIVSILDK	45
		TVSEWLESIK	25
Src	P12931	AANILVGENLVCK	54
Cortactin	Q14247	VDQSAVGFEYQGK	44
		YGLFPANYVELR	84
p130 Cas	P56945	LVFIGDTLSR	33
		ATAPGPEGGGTLHPNPTDK	20
SHEP1	Q8N5H7	TEGTK	30
		LDLLER	39
PTP-PEST	Q05209	TLLLEFQNESR	55
RIL	P50479	GYFFLDER	46
		DFSAPLTISR	25
		VKPPEGYDVVAVYPNAK	17
Lasp1	Q14847	GFSVVADTPELQR	60
SNAP23	O00161	ILGLAIESQDAGIK	76
FHL2	Q14192	CSLSLVGR	59
		YISFEER	43
		NSLVDKPFAAK	24
		CAGCTNPISGLGGTK	26
		GSSWHETCFICHR	54
		DDFAYCLNCFCDLYAK	61
		EDQLLCTDCYSNEYSSK	29
HAX1	O00165	IFGGVLESDAR	38
adducin	P35611	INLQGDIVDR	49
MARCKS	P29966	LSGFSFK	31
		GEPAAAAAPEAGASPVEK	26
		EAPAEGEAAEPGSPTAAEGEA ASAASSTSSPK	86
Gelsolin	P06396	AGALNSNDAFVLK	41
Integrin alpha-3	P26006	YLLLAGAPR	23
		TVEDVGSPLK	34
		LELLLMDNLR	26
		LELLLMDNLR	41
		EAGNPGSLFGYSVALHR	27
Integrin beta-1	P05556	IGFGSFVEK	64
		LLVFSTDAGFHFAGDGK	63

Lévêque *et al.*, Figure 1

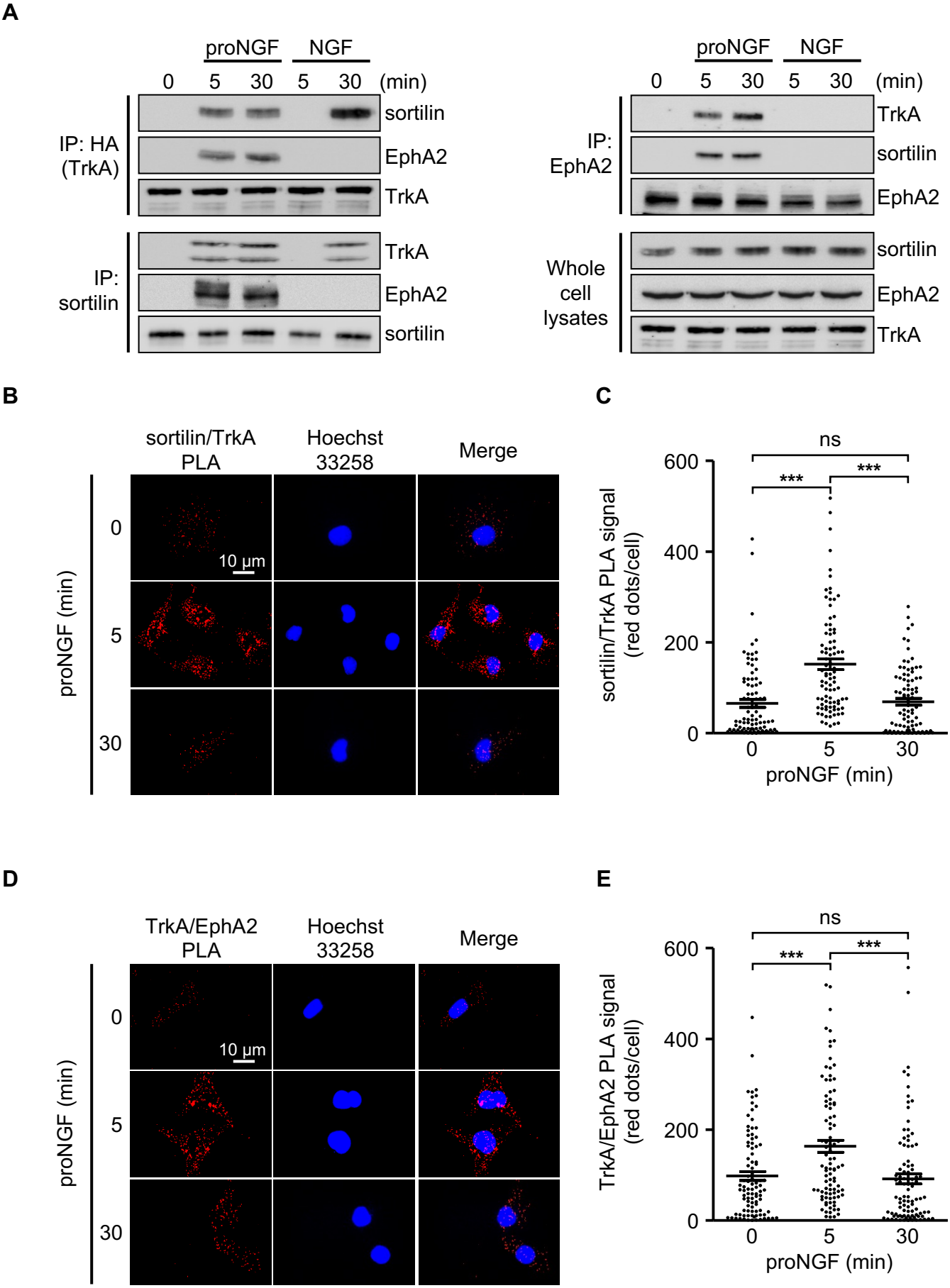

Lévêque *et al.*, Figure 2

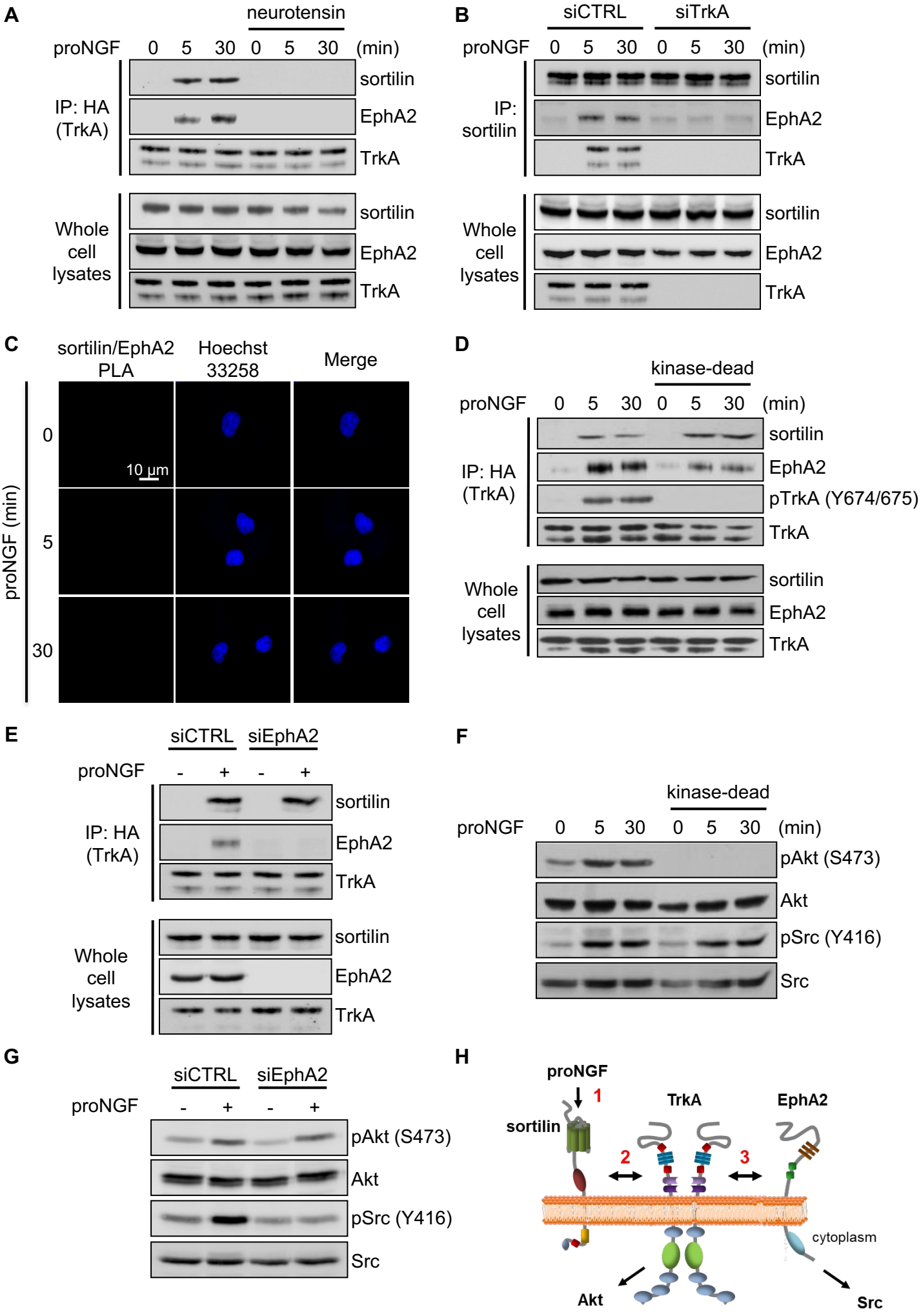

Lévêque *et al.*, Figure 3

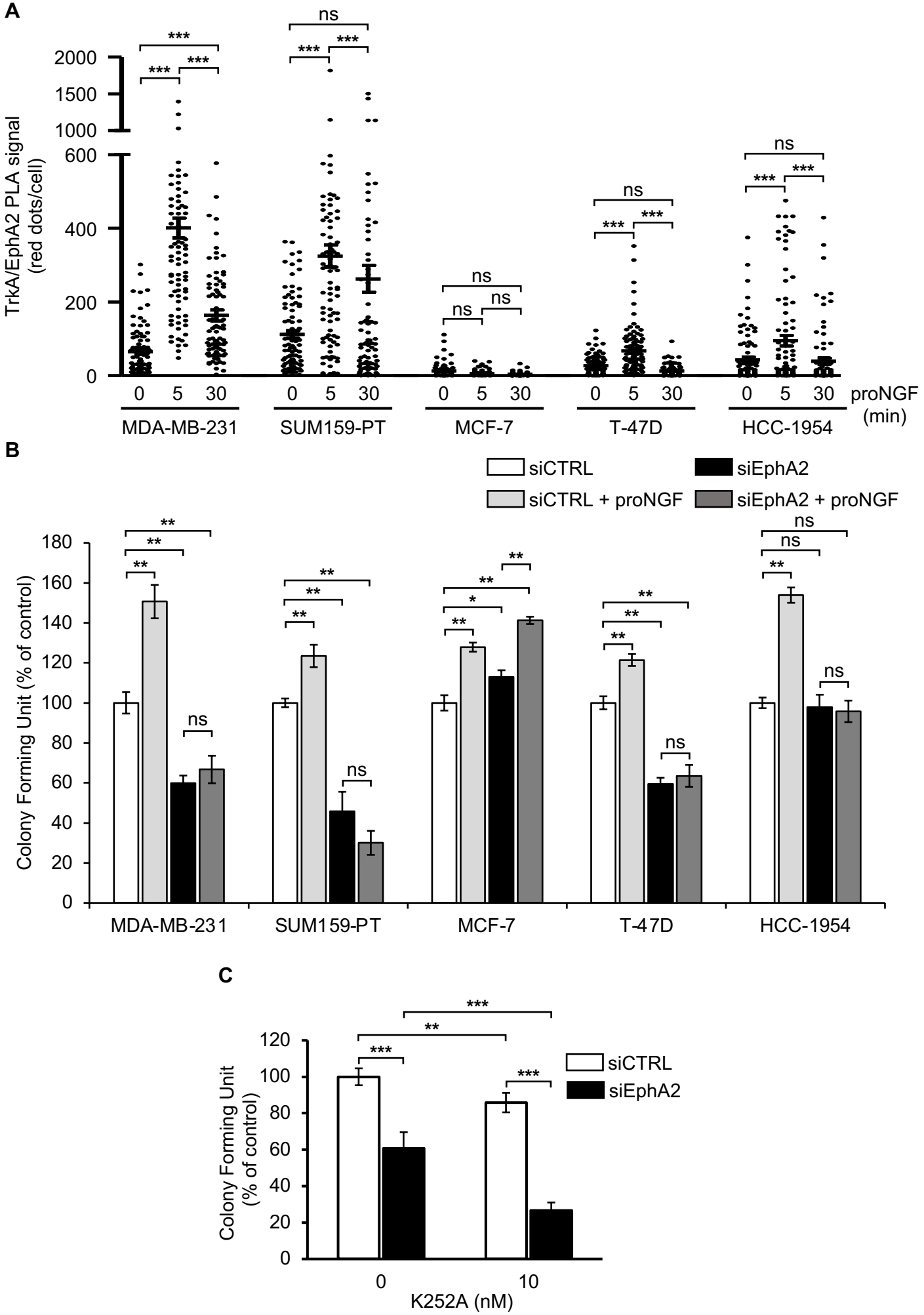

Lévêque *et al.*, Figure 4

A

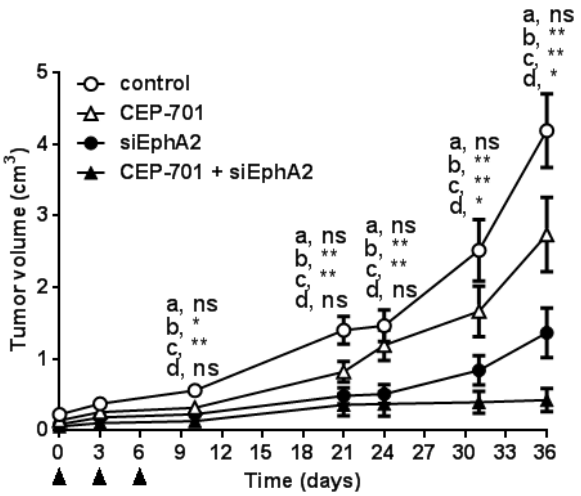

B

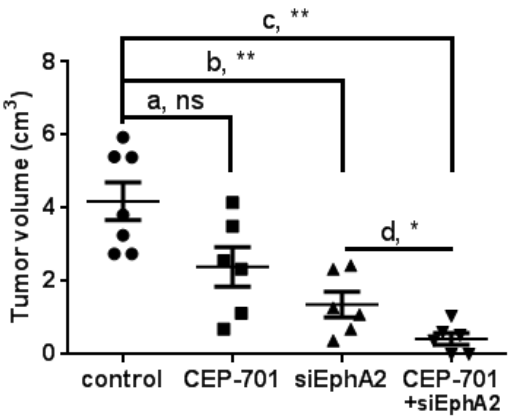

C

Metastasis in mice	siCTRL	siTrkA	siEphA2	siTrkA+siEphA2
Lung	10/10	10/10	10/10	10/10
Liver	7/10	4/10	7/10	4/10
Brain	8/10	8/10	7/10	4/10

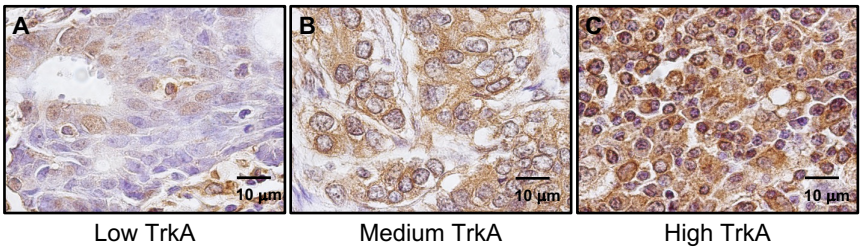

Low TrkA | Medium TrkA | High TrkA

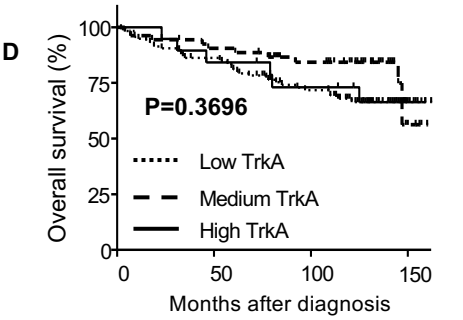

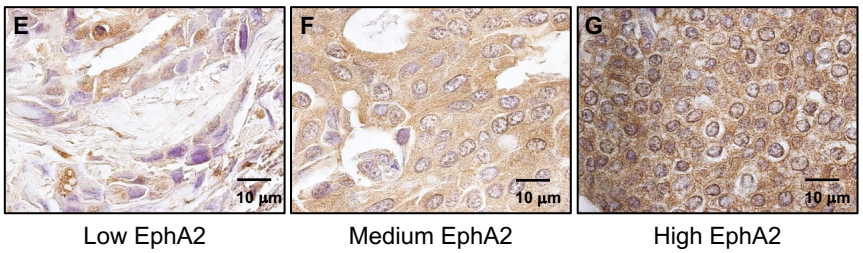

Low EphA2 | Medium EphA2 | High EphA2

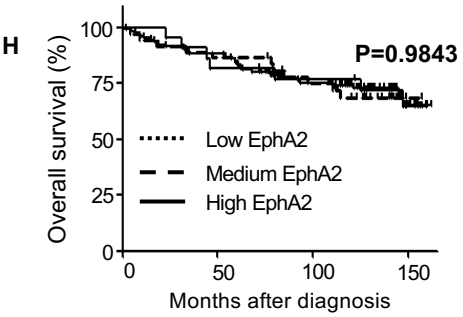

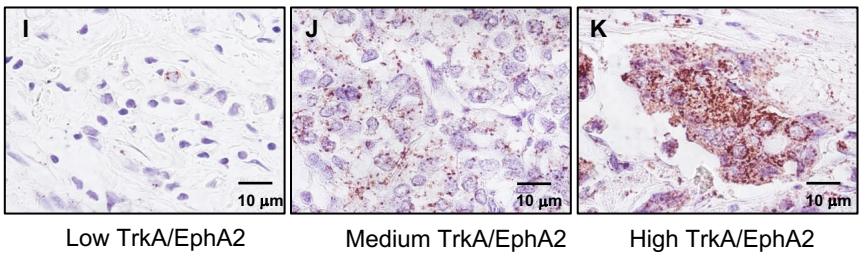

Low TrkA/EphA2 | Medium TrkA/EphA2 | High TrkA/EphA2

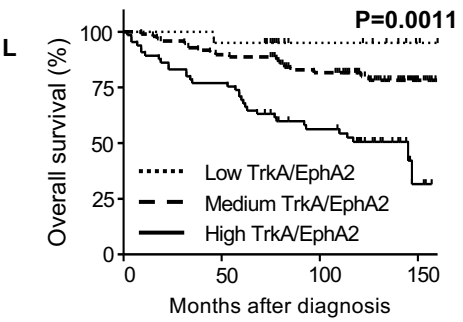

Lévêque *et al.*, Figure 6

ProNGF increases breast tumor aggressiveness through functional association of TrkA with Ephrin type-A receptor 2

Lévêque Romain, Corbet Cyril, Aubert Léo, Guilbert Matthieu, Lagadec Chann, Adriaenssens Eric, Duval Jérémy, Finetti Pascal, Birnbaum Daniel, Magné Nicolas, Chopin Valérie, Bertucci François, Le Bourhis Xuefen & Toillon Robert-Alain

SUPPLEMENTARY FIGURE LEGENDS

Supplementary Figure S1: Efficacy of siTrkA.

Representative Immunoblotting for HA (TrkA) in HA-TrkA MDA-MB-231 cells transfected with control, three different TrkA-targeting siRNAs or a pool of the three TrkA-targeting siRNAs.

Supplementary Figure S2: ProNGF-induced invasion is dependent of EphA2.

Native and HA-TrkA MDA-MB-231 cells were transfected EphA2-targeting siRNA were seeded in collagen coated Boyden chambers and treated with non-cleavable proNGF (0.5nM) or NGF (16nM) for 16 hours. Invading cells were then counted and results were reported as a percentage of invading cells compared to control. Data are expressed as means ± SEM. **p<0.01; ns, not significant.

Supplementary Figure S3: Representative pictures for sortilin/EphA2 PLA in wild-type MDA-MB-231 (**A**), SUM159-PT (**B**), MCF-7 (**C**), T-47D (**D**) and HCC1954 (**E**) cells. Cells were treated with non-cleavable proNGF (0.5 nM) for 5 or 30 min and then subjected to TrkA/EpHA2 PLA staining.

Supplementary Figure S4: Representative western blots for TrkA and EphA2 expression in wild-type MDA-MB-231, SUM159-PT, MCF-7, T-47D and HCC1954 cells.

Supplementary Figure S5: Efficacy of another siEphA2. (**A**) Clonogenic cell growth of MDA-MB-231 cells following non-cleavable proNGF treatment and transfection of EphA2-targeting siRNA. Data are expressed as means ± SEM. **p<0.01; ns, not significant. (**B**) Representative pictures of clonogenic growth.

Supplementary Figure S6: Kaplan-Meier OS curves in mice according to siCTRL, siTrkA, Si EphA2 and combinatory siTrkA and siEphA2 treatments. Xenograft experiments were conducted using MDA-MB-231 HA-TrkA cells. The tumors were allowed to develop for 14 days and the mice were then submitted to 5 injections (every 3 days) of either scrambled siRNA, or TrkA- and EphA2-targeting siRNAs alone or in combination (7.5 µg siRNA/mouse). Tumor volume was determined throughout the experiment by measuring the length (l) and width (w) and tumors were allowed to grow up to 2 cm^3 to allow metastasis of cancer cells and mice were sacrificed in accordance with ethical pratices.

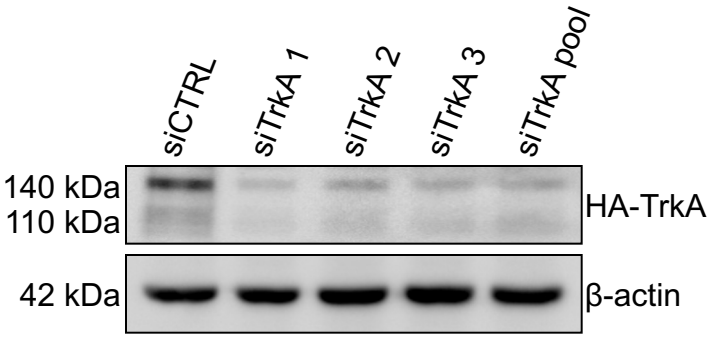

Lévêque *et al.*, Figure S1

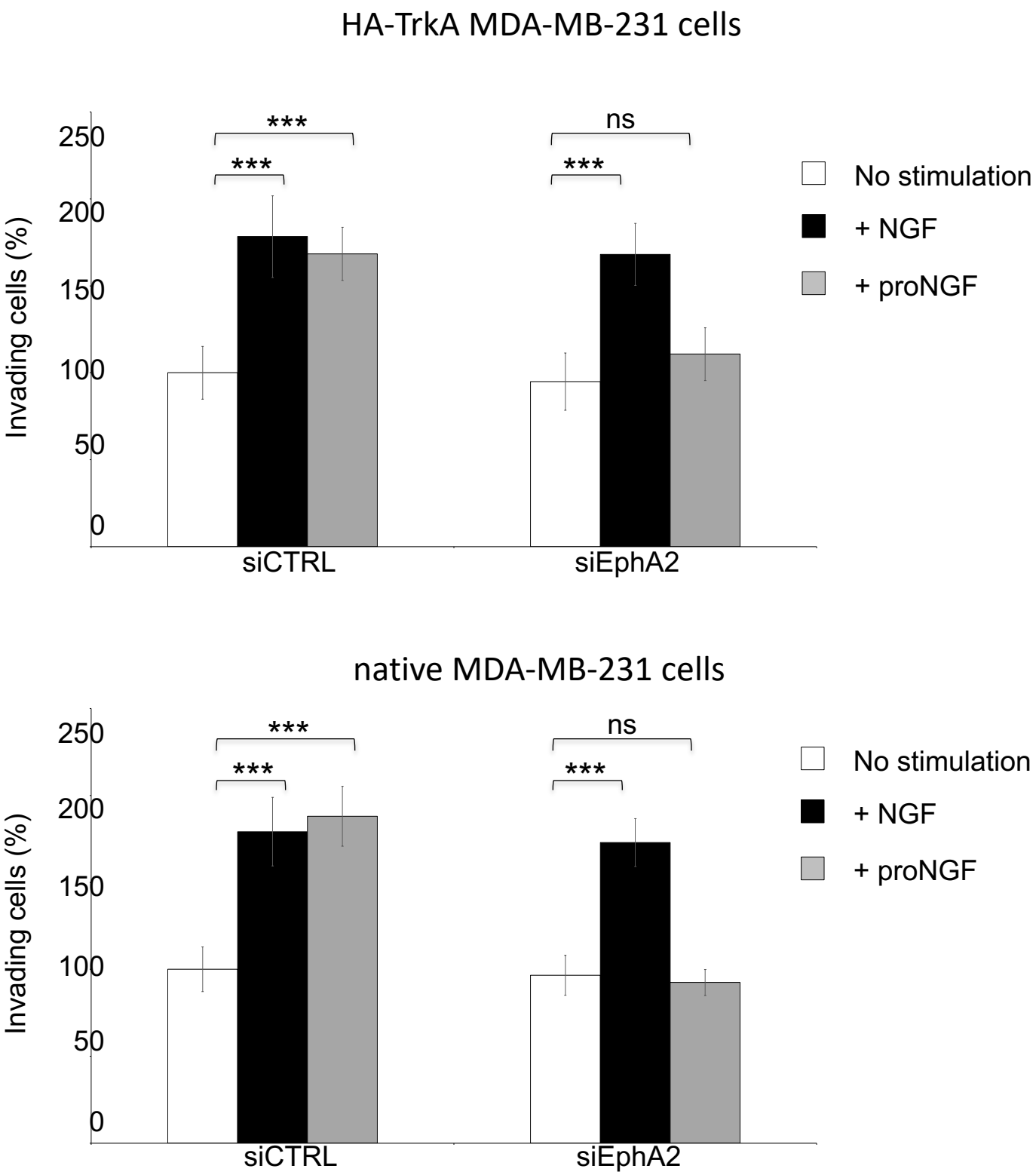

Lévêque *et al.*, Figure S2

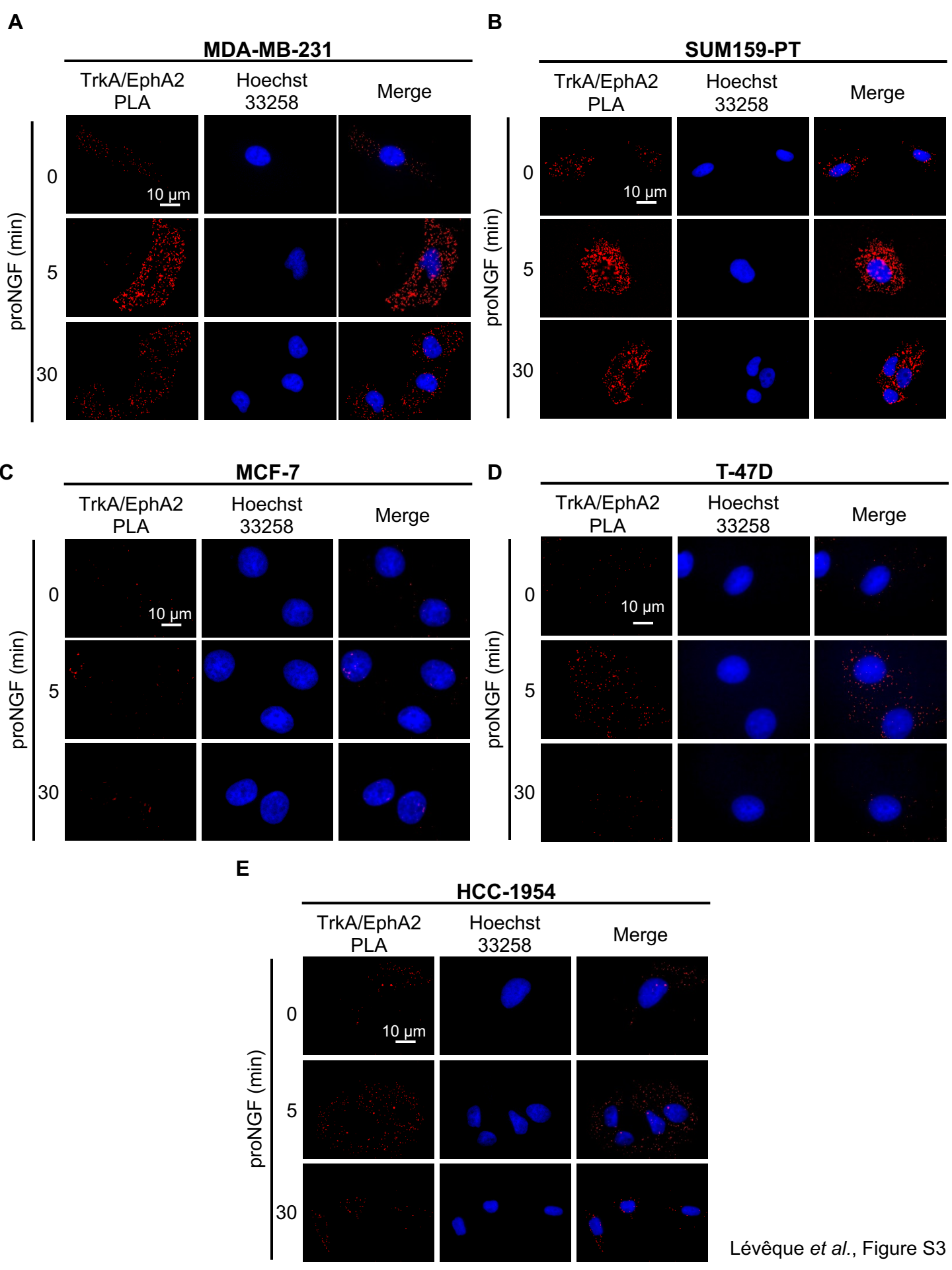

Lévêque *et al.*, Figure S3

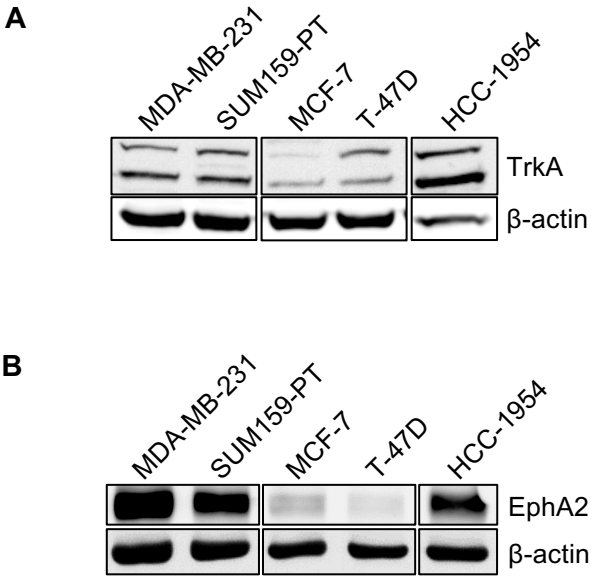

Lévêque *et al.*, Figure S4

A

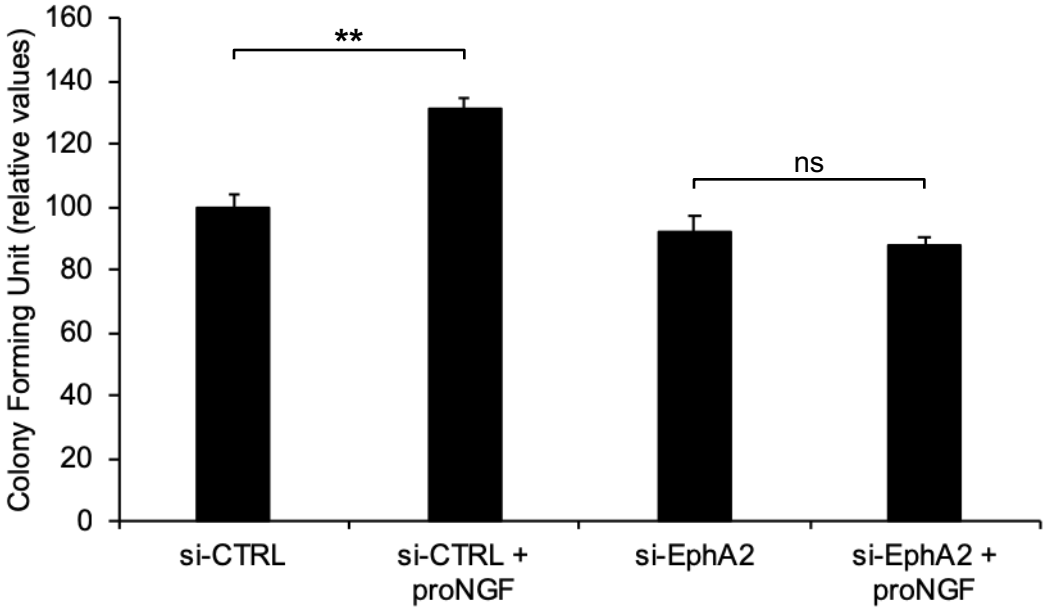

B

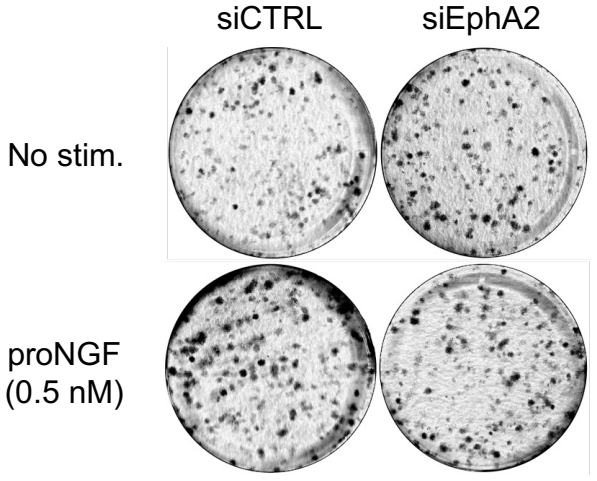

Lévêque *et al.*, Figure S5

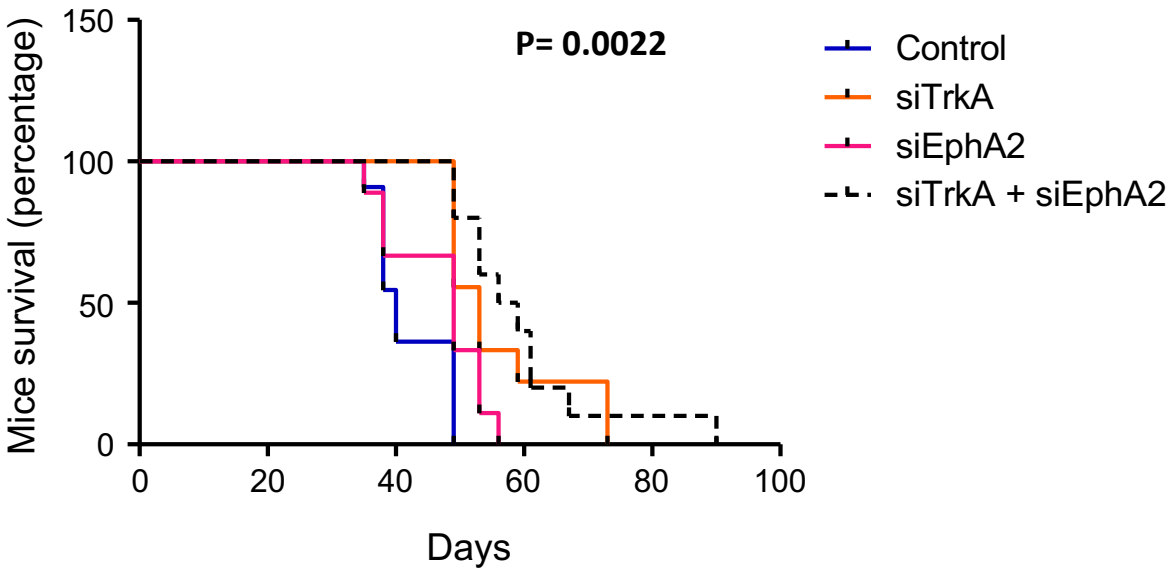

Lévêque *et al.*, Figure S6